



# Absorption and Diffusion Measurements of Biological Samples using a THz Free Electron Laser

E. GIOVENALE, M. D'ARIENZO, A. DORIA, G.P. GALLERANO, A. LAI,  
G. MESSINA and D. PICCINELLI

*ENEA C.R. Frascati – V. E. Fermi 45 – 00044 Frascati, Italy*

**Abstract.** A compact THz Free Electron Laser (FEL) is being used to perform irradiation of biological samples to investigate possible genotoxic effects. In order to evaluate the exact radiation dose absorbed by the single components of the samples it is necessary to study the optical properties of the samples, separating the contributions to the radiation attenuation coefficient coming from absorption and from diffusion. Spectroscopic measurements have been performed on different biological samples, comparing the experimental results with theoretical models.

**Key words:** Biological effects, blood, Free Electron Laser, lymphocytes, THz radiation

## 1. Introduction

ENEA is presently coordinating an EU project, called THz-BRIDGE, devoted to the study of the effects of THz radiation on biological samples. Experimental measurements conducted on systems of increasing complexity are being performed, and the parameters of the irradiation, like incident and absorbed power, wavelength, pulse duration and modulation conditions, are taken into account in order to evaluate and identify the possible biological effect. This will provide a risk assessment prior to the future implementation of THz devices in bio-medical diagnostics. Genotoxic effects are one of the most interesting aspects in the risk assessment of human exposure to ionizing and non-ionizing electromagnetic radiation, due to the close correlation between DNA damage and cancer occurrence. In this work human lymphocyte cultures are being used as a biological model for studying potential genotoxic effects. Lymphocytes are a well-known biological system playing a key role in the defence mechanisms; they are the only blood constituents with a nucleus and they are semi-synchronised cells easily obtainable from peripheral blood and can be stimulated to divide *in vitro* by a variety of substances (mitogens). Cytogenetic techniques allow one to test DNA damage, at cellular and molecular level, induced by various chemical and physical agents. The cytokinesis-block mi-

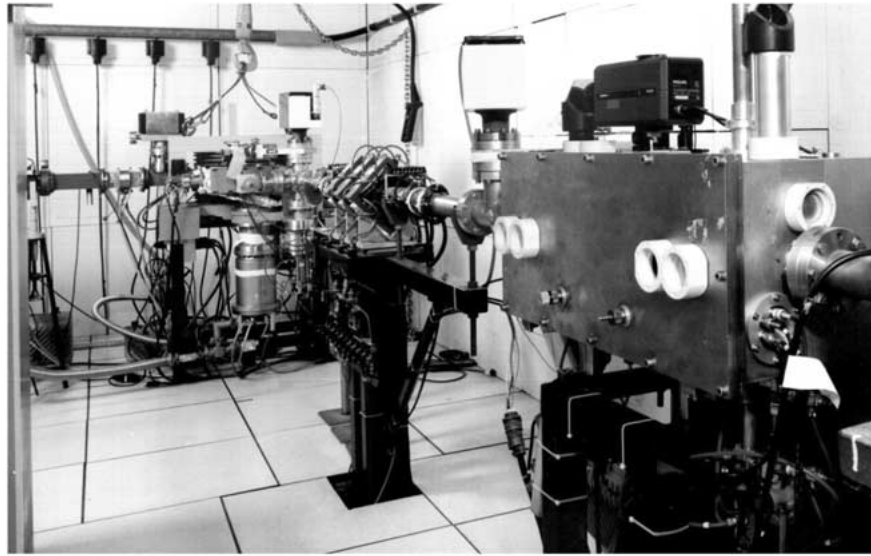


Figure 1. The ENEA Compact FEL Layout.

Table I. FEL operation parameters

|                                |      |                           |        |
|--------------------------------|------|---------------------------|--------|
| Electron Energy (MeV)          | 2.3  | Und. period (cm)          | 2.5    |
| I-peak (A)                     | 4    | N (num. of periods)       | 8      |
| I-av (A)                       | 0.2  | Undulator par. K          | 1      |
| Micropulse duration (ps)       | 15   | Wavelength (mm)           | 2.6    |
| Macropulse duration ( $\mu$ s) | 4    | Tuning range (mm)         | 2–3    |
| Norm. emittance (cm rad)       | 0.02 | Bandwidth                 | 0.6–8% |
| Energy spread                  | 1%   | $P_{out} - 4\mu$ s – (kW) | 1.5    |

chromosome technique (MN) is a very sensitive and simple indicator of chromosome damage, which also provides information on cell cycle progression [1].

To study such potential genotoxic effects, whole blood samples are being exposed primarily to millimetre-wave (mm-wave) radiation generated by a Free Electron Laser (FEL) available at ENEA [2]. This source operates in the spectral range between 70 and 200 GHz with a peak power in the kW range and a particular temporal structure of the pulses. In order to correctly evaluate the dose delivered to the sample a complete theoretical and experimental description of the optical properties of the blood and of its constituents is necessary.

In this work both theoretical calculations and experimental measurements are reported regarding the absorption properties of blood and blood constituents. Results have been utilised for a better understanding of the irradiation measurements.

## 2. The Source

The source used for both absorption measurements and irradiation is a compact mm-wave free electron laser, operating at the ENEA center of Frascati (Figure 1). In a Free Electron Laser (FEL) a beam of high energy electrons interacts with a suitable magnetic structure (undulator) to generate coherent electromagnetic radiation. The ENEA compact FEL utilizes a Microtron as electron source, with electron energy ranging from 2.3 MeV and 5 MeV. The system is very flexible, allowing the use of different interaction structures to produce radiation: permanent magnets undulators [3], Cherenkov FEL structures [4] and metal grating structures (Smith-Purcell FELs) [5]. Such a flexibility is reflected by the wide spectral range of the emission, from a few hundred micrometers, up to a few millimeters. In our irradiation experiments an undulator has been used, in order to obtain a strong peak emission in the spectral range around 120 GHz ( $\lambda = 2.5$  mm). The absorption measurements have then been conducted in the same spectral region. In Table I the FEL parameters used for the measurements discussed in this article are reported.

As mentioned in the introduction, another interesting feature of the source used is related to the peculiar temporal characteristics of the RF driven FEL emission. Emission is composed of a train of pulses (called macropulses), that in our system are 4  $\mu$ s long, with a repetition frequency up to 20 Hz. Inside the macropulses a further structure is present, with very short ‘micropulses’, spaced by the driving radiofrequency period. In our system the microtron driving radiofrequency is 3 GHz, so that the micropulse structure is composed of 50 ps micropulses, spaced apart by 330 ps ( $1/\nu_{RF}$ ). This particular temporal structure of the emitted radiation allows the investigation of the effects of very high peak power, while maintaining a low average power delivered to the sample, thus avoiding heating effects.

A maximum output power of about 1.5 kW in 4  $\mu$ s pulses has been obtained at 120 GHz.

The spectral features of the Compact FEL operating at 120 GHz at maximum power are shown in Figure 2, where three interferometric orders of a high finesse ( $F = 200$ ) Fabry-Perot interferogram are reported. The spectrum consists of several emission lines, spaced at 3 GHz intervals, which are due to the periodic structure of the electron pulses. The envelope of the emission lines shows a relative bandwidth that can be varied between 0.6% and 8% bandwidth depending on the FEL operation parameters.

The FEL radiation is transported to a dedicated user room by means of a special mm-wave transmission line composed of an evacuated copper light pipe with 25 mm clear aperture and appropriate delivery optics. A variety of detectors, including a Ge:Ga photoconductor, an InSb electron bolometer, fast pyroelectric detectors and a power meter are available to characterize the FEL performance in the wavelength spectral range from 50  $\mu$ m to several millimeters.

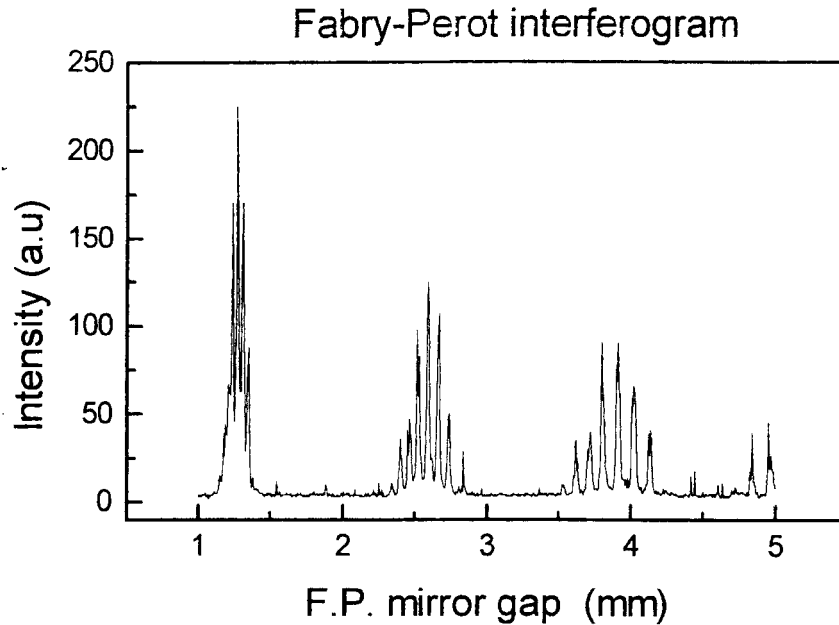


Figure 2. Fabry-Perot interferogram of the FEL radiation. The first three interference orders are visible. The discrete structure of the RF driven FEL emission is evident.

### 3. The Absorption Measurements

An important consideration concerning the study of the absorption of THz radiation in biological systems, and more specifically in whole blood, is that, at these frequencies, the macroscopic structure of the sample components must be taken into account for a proper modeling of the interaction. In fact whole blood can be considered as a colloidal dispersion of blood-cells into the plasma. Blood-cells are small (typically  $10 \mu\text{m}$  diameter) when compared to the radiation wavelength, but not small enough to be neglected while evaluating the homogeneity of the blood sample. As a consequence, a correct study of the interaction mechanism must consider the wave propagation in a disordered medium where the blood-cells act as scattering elements. In the approximation of weak scattering the cells can be treated as rigid dielectric particles with a small difference in the refractive index with respect to the medium. The diffusive properties have then to be considered together with the absorption characteristics of the medium. Absorption at THz frequencies is mainly due to the water content of the plasma. When an electromagnetic wave propagates through such a medium its intensity is attenuated according to the absorption and diffusion laws respectively:

$$I_T = I_0 \exp(-\alpha x) \quad (1a)$$

$$I_D \propto I_0/x \quad (1b)$$

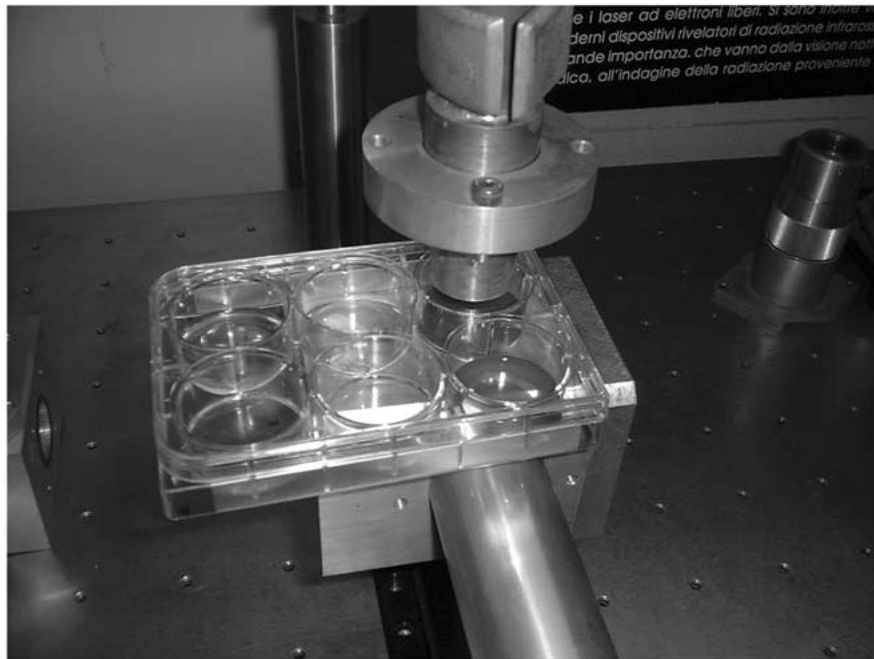


Figure 3. Spectral measurements setup: radiation from the vertical copper light-pipe impinges on the sample in the Petri dish. The transmitted radiation is reflected by a metal mesh mirror and measured with a pyroelectric detector.

where  $I_0$ ,  $I_T$ ,  $I_D$ , are the intensities of the incident, transmitted and diffused wave respectively,  $x$  is the distance the wave covers through the medium and  $\alpha$  is the absorption coefficient of the medium.

The penetration depth of the Compact FEL radiation through various biological samples has been measured at 120 GHz to determine the most efficient way to obtain a uniform exposure during the irradiation of whole blood. Absorption measurements have been carried out on whole human blood, serum, plasma, water, saline solution, culture medium, lymphocytes, and other biological samples. Absorption measurements have also been carried out on materials to be used as a container for the biological samples, like polystyrene and polyethylene. Polystyrene has been found to exhibit good optical properties in the spectral region around 120 GHz, and was thus selected as the material for spectroscopic cells.

Radiation transported into the control room by the 25 mm diameter light pipe was delivered to the biological sample, contained in a polystyrene Petri dish. The radiation transmitted through a 13 mm hole under the sample impinges on a 45° mirror and is finally collected by a pyroelectric detector (Figure 3). Results of raw absorption measurements are reported in Figure 4. It is easy to see that the transmission exhibits an exponential decay as a function of the sample thickness,

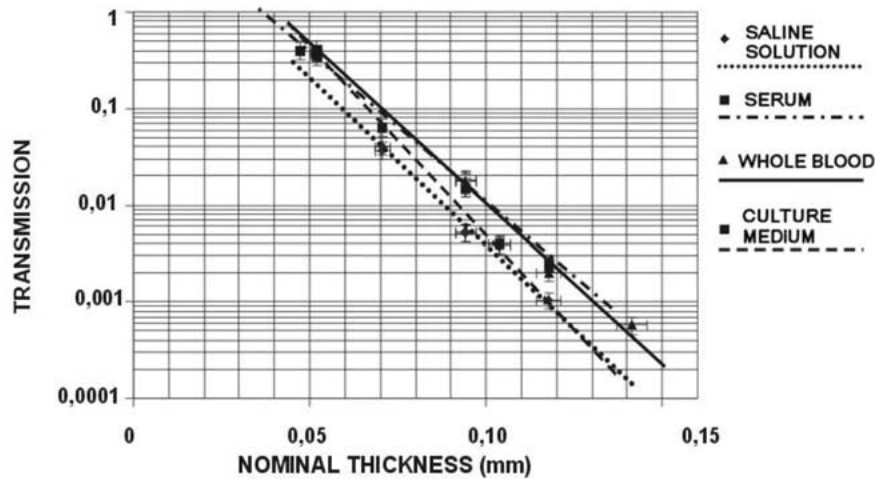


Figure 4. Transmission data for different biological samples.

Table II. Absorption coefficient for different biological samples

| Sample          | $\alpha$ (cm <sup>-1</sup> ) |
|-----------------|------------------------------|
| Blood           | 75 ± 3                       |
| Serum           | 71 ± 3                       |
| Saline solution | 79 ± 3                       |
| Culture medium  | 83 ± 3                       |

thus confirming that the ballistic regime prevails over the diffusive one at these wavelengths.

This result confirms the theoretical calculations based upon the Mie diffusion theory [6] that gives a scattering cross section several orders of magnitude lower than the absorption cross section at these wavelengths for blood and blood components in different host solutions. According to calculations the diffusive contribution to the extinction cross section can be higher at shorter wavelengths. From the angular coefficient of the lines interpolating the experimental data the absorption coefficients of the different samples were calculated and are reported in Table II.

It is easy to observe from the graphs in Figure 4, that the interpolated lines do not intercept the  $x = 0$  axis at the theoretical value 1. This is due to the sum of two different effects. On one hand the reflection from the sample surface reduces the intensity of the radiation entering the sample, thus producing a lower value for the observed transmission. On the other hand, due to the surface tension of the liquid samples, a 'meniscus' effect is observed because the liquid 'sticks' to the side surfaces of the polystyrene container, thus reducing the effective thickness of

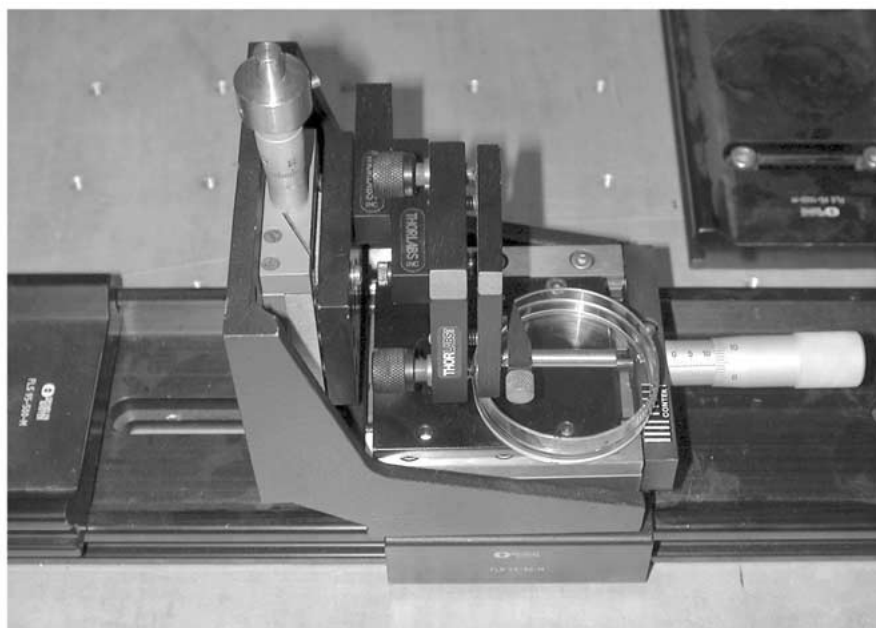


Figure 5. Layout of the system utilised to measure the surface meniscus in different liquids.

the sample at the center of the container, where the transmission is measured. As a result of the lower effective thickness, a higher transmission value is observed. The two effects rigidly 'move' the lines in opposite directions. As can be observed from Figure 4 the meniscus effect is the prevailing one.

In order to obtain data about the reflection properties of the samples it is thus necessary to measure the exact value of the sample thickness. This has been done using the system shown in Figure 5.

A two axis motion system, equipped with a sharp needle, has been used to 'map' the shape of the sample surface, with an accuracy of  $5 \mu\text{m}$ . Measurements have been performed in different radial directions, in order to verify the uniformity of the system. Results are shown in Figure 6.

Once the exact sample surface profile is known, it is easy to calculate the effective sample thickness and thus correct the transmission graph. The corrected graphs are reported in Figure 7. From these graphs it is possible to evaluate the reflected radiation intensity.

It is thus possible to obtain the value of the real and of the imaginary part of the refractive index of the different samples.

It is interesting to notice that the optical parameter obtained from our measurements are consistent with the results obtained utilizing the semi-empirical Cole-Cole formula [7]:

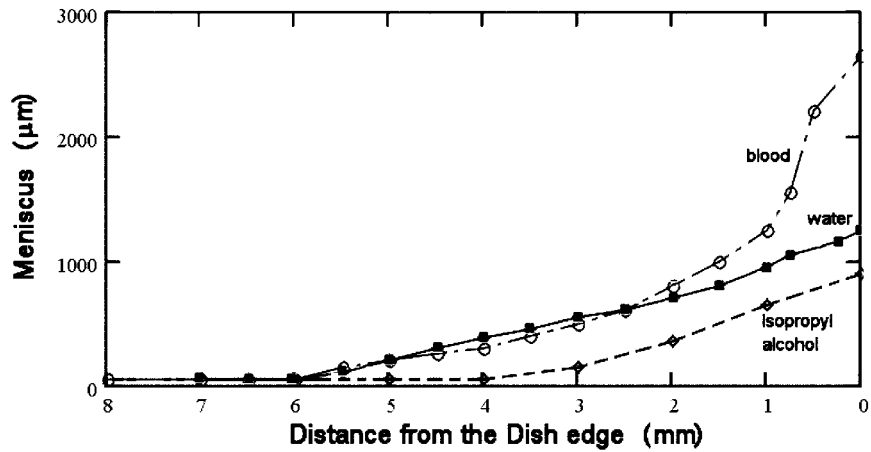


Figure 6. ‘Meniscus’ measurements for different samples: blood (○), water (□), isopropyl alcohol (◇).

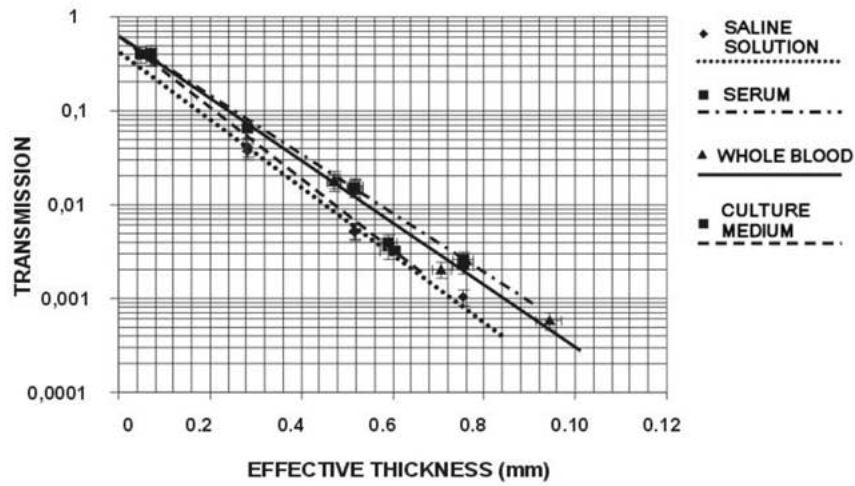


Figure 7. Transmission data for different biological samples, corrected taking into account the ‘meniscus effect’.

$$\varepsilon(\omega) = \varepsilon_{\infty} + \sum_{n=1}^4 \frac{\Delta\varepsilon_i}{1 + (i\omega\tau_i)^{1-\alpha_i}} + \frac{\sigma}{i\omega\varepsilon_0} \quad (2)$$

Where the value for  $\alpha_i$ ,  $\Delta\varepsilon_i$ , and  $\tau_i$  are obtained from a linear regression, starting from experimental data taken in different frequency regions [8].

These data can then be used to exactly calculate the power density at a certain depth within the sample, where lymphocytes are localized.

Human blood, once put into the Petri dishes, tends to form a sediment, and after about 20 minutes it is possible to distinguish three different ‘layers’. The upper



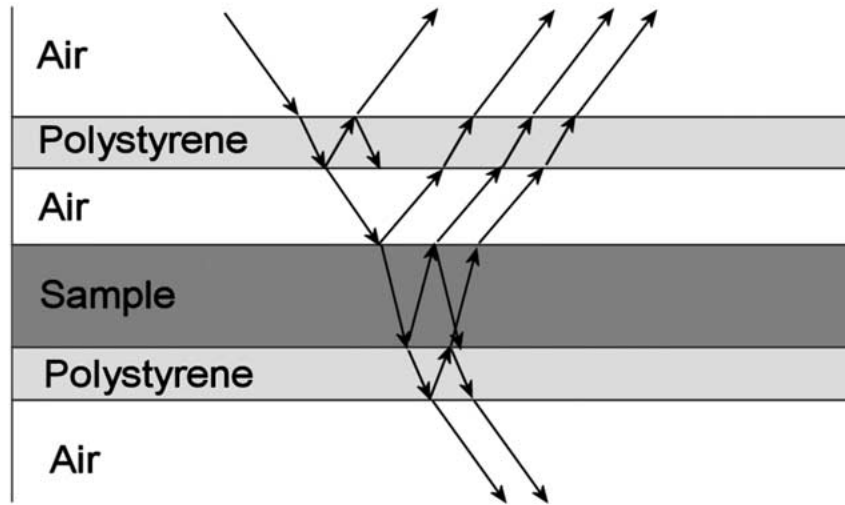


Figure 8. Six-layer model for irradiation measurements.

layer is mainly composed by serum, while the lower layer is made of sedimented erythrocytes. Between the two main layers, each about 50% of the total volume, a very thin layer is visible, containing the lymphocytes. It is thus necessary to evaluate the intensity of the radiation that effectively impinges on the lymphocytes. To perform this task a model has been utilized, where the reflections on the interfaces between different layers are taken into account [9]. In our case a 6-layer model has been used as shown in Figure 8: air-polystyrene-air-sample-polystyrene-air. The sample is considered as a single layer, since erythrocytes can be considered as lipid membranes full of water, so that the absorption properties are very similar to those of the whole blood. This assumption has been confirmed by calculations based upon the Mie theory, considering 4  $\mu m$  diameter lymphocytes with a lipid non-absorbing membrane of about 0.3  $\mu m$ .

In Figure 9 the transmitted intensity as a function of the depth inside the sample, for different values of the sample thickness  $d$  is reported. From these data it is possible to calculate the value of the electric field inside the samples, given by

$$E(x) = \sqrt{\frac{P(x)}{\omega \epsilon_0 \epsilon_{imm} V}} \tag{3}$$

Where  $\epsilon_{imm}$  for the sample has been calculated from the absorption coefficient to be  $\epsilon_{imm} = 10$ .

In Table III the values of the electric field on the lymphocytes are reported, for the average power, the peak power over the 4  $\mu s$  pulse and the peak power over the 50 ps micropulses.

Once the emission intensity on the lymphocytes is known, it is important to evaluate how much radiation is absorbed by the lymphocytes. From the absorption

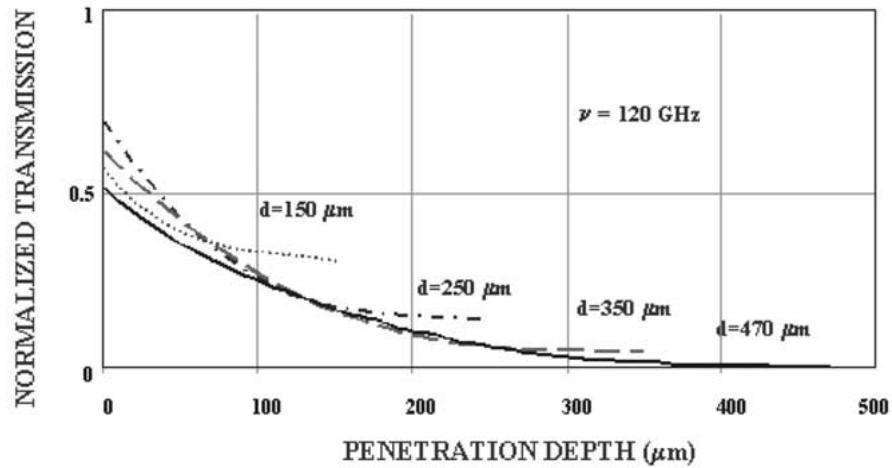


Figure 9. Graph of the transmission at different depth inside the sample, for different values of the sample thickness:  $d = 150 \mu\text{m}$  (.),  $d = 250 \mu\text{m}$  (-.-.-),  $d = 350 \mu\text{m}$  (- - -),  $d = 470 \mu\text{m}$  (—). For thin samples multiple reflections inside the system increase the overall transmission.

Table III. Calculation of the Electric field on the lymphocytes

|                  | $\langle P \rangle_{120\text{GHz}}$ | $\hat{p}_{4\mu\text{s}}^{120\text{GHz}}$ | $\hat{p}_{50\text{ps}}^{120\text{GHz}}$ | $\langle P \rangle_{130\text{GHz}}$ | $\hat{p}_{4\mu\text{s}}^{130\text{GHz}}$ | $\hat{p}_{50\text{ps}}^{130\text{GHz}}$ |
|------------------|-------------------------------------|--|---|-------------------------------------|--|---|
| Power impinging  |                                     |  |   |                                     |  |   |
| on the sample    | 1 mW                                | 125 W                                    | 825 W                                   | 0.6 mW                              | 75 W                                     | 495 W                                   |
| E on lymphocytes | 8.3 V/m                             | 2.9 kV/m                                 | 7.6 kV/m                                | 6.4 V/m                             | 2.3 kV/m                                 | 5.8 kV/m                                |

measurements it is evident that the high water content of the biological material produces a very high absorption, which makes it very difficult to evaluate the absorption contribution of the lymphocytes. It is thus necessary to find a different host solution, with low absorption in the region of interest, in order to verify if lymphocytes show a resonant absorption around 120 GHz. The absorption of different alcoholic liquids has been measured in order to find the best candidate as host solution for lymphocytes. Results are reported in Table IV.

Isopropyl alcohol has been identified to be the best candidate for direct absorption measurements on lymphocytes. The main limitation is due to the fact that isopropyl alcohol is not isotonic with lymphocytes. Thus, after a short time, death of the cell is observed. From direct microscopic observations it has been noted that survival time for lymphocytes in isopropyl alcohol is about 15 minutes. This time is sufficient to correctly perform the absorption measurements. Utilizing a lymphocyte concentration similar to the normal lymphocyte concentration in blood, no changes in the absorption at 120 GHz has been observed. This means that the lymphocyte absorption is below the measurement sensitivity ( $\alpha = 0.5 \text{ cm}^{-1}$ ), as

Table IV. Absorption coefficient of different alcoholic liquids

|                   | $\alpha$ (cm <sup>-1</sup> ) |
|-------------------|------------------------------|
| Isopropyl Alcohol | 5.0 ± 0.5                    |
| Ethyl Alcohol     | 11.0 ± 0.5                   |
| Alcoholic Soda    | 13.0 ± 0.5                   |

predicted using the Mie theoretical model, and that there is no evidence of resonant absorption in the spectral region of interest.

Further measurements will be conducted utilizing higher lymphocytes concentrations in order to precisely evaluate the absorption coefficient.

#### 4. Conclusions

Spectroscopic measurements have been conducted to obtain the optical properties of human blood and blood components in the spectral region around 120 GHz. These data have been used to calculate the value of the electric field when irradiating whole human blood to verify potential cytotoxic effects, thus delivering exact data correlating the field intensity to the observed effects.

#### Acknowledgements

This paper has been carried out with financial support from the Commission of the European Communities, specific RTD programme 'Quality of Life and Management of Living Resources', QLK4-2000-00129 'Tera-Hertz Radiation In Biological Research, Investigation on Diagnostics and study on potential Genotoxic Effects'. It does not necessarily reflect its view and in no way anticipates the Commission's future policy in this area.

#### References

1. Fenech, M.: The Cytokinesis-Block Micronucleus Technique: A Detailed Description of the Method and its Application to Genotoxicity Studies in Human Population, *Mutation Res.* **285** (1993), 35–44.
2. Gallerano, G.P., Doria, A., Giovenale, E. and Renieri, A.: Compact Free Electron Lasers: From Cherenkov to Waveguide Free Electron Lasers, *Infrared Phys. and Tech.* **40** (1999), 161–174.
3. Ciocci, F., Bartolini, R., Doria, A., Gallerano, G.P., Giovenale, E., Kimmitt, M.F., Messina, G. and Renieri, A.: Operation of a Compact Free-Electron Laser in the Millimeter-Wave Region with a Bunched Electron Beam, *Phys. Rev. Lett.* **70** (1993), 928–931.
4. Ciocci, F., Doria, A., Gallerano, G.P., Giabbai, I., Kimmitt, M.F., Messina, G. and Renieri, A.: Observation of Coherent Millimeter and Submillimeter Emission from a Microtron-Driven Cherenkov Free-Electron Laser, *Phys. Rev. Lett.* **66** (1991), 699–702.

5. Doucas, G., Kimmitt, M.F., Doria, A., Gallerano, G.P., Giovenale, E., Messina, G., Andrews, H.L. and Brownell, J.H.: Determination of Longitudinal Bunch Shape by Means of Coherent Smith-Purcell Radiation, *Phys. Rev. STAB* **5** (2002), 072802.1–072802.8.
6. Van De Hulst, H.C.: *Light Scattering by Small Particles*, Dover, 1981.
7. Cole, K.S. and Cole, R.H.: Dispersion and Absorption in Dielectrics: I. Alternating Current Characteristics, *J. Chem. Phys.* **9** (1941), 341–351.
8. Gabriel, C., Gabriel, S. and Corthout, E.: The Dielectric Properties of Biological Tissues: III. Parametric Models for the Dielectric Spectrum of Tissues, *Phys. Med. Biol.* **41** (1996), 2271–2293.
9. Born, M. and Wolf, E.: *Principles of Optics*, Pergamon Press, Oxford, 1975.